Quantification of muscle coordination underlying basic shoulder movements using muscle synergy extraction

Umehara, Jun; Yagi, Masahide; Hirono, Tetsuya; Ueda, Yasuyuki; Ichihashi, Noriaki

J Biomech. 2021 May 7;120:110358
doi: 10.1016/j.jbiomech.2021.110358

Quantification of muscle coordination underlying basic shoulder movements using muscle synergy extraction

Jun Umehara[abc], Masahide Yagi[a], Tetsuya Hirono[ab], Yasuyuki Ueda[ad], Noriaki Ichihashi[a]

[a] Human Health Sciences, Graduate School of Medicine, Kyoto University, Kyoto, Japan

[b] Research Fellow of Japan Society for the Promotion of Science, Tokyo, Japan

[c] Center for Information and Neural Networks (CiNet), National Institute of Information and Communications Technology, Osaka, Japan

[d] Department of Rehabilitation, Nobuhara Hospital, Hyogo, Japan

Abstract

Numerous muscles around the shoulder joint are required to work in a coordinated manner, even when a basic shoulder movement is executed. Muscle synergy can be utilized as an index to determine muscle coordination. The purpose of the present study was to investigate the muscle coordination among different shoulder muscles underlying basic shoulder movements based on muscle synergy. Thirteen men performed 14 multiplanar shoulder movements; five movements were associated with elevation and lowering, while five were associated with horizontal abduction and adduction. The four additional movements were simple rotations at different positions. Muscle activity was measured from 12 muscle portions using surface electromyography. Using the dimensionality reduction technique, synergies were extracted first for each movement separately (“separate” synergies), and then for the global dataset (containing all movements; “global” synergies). The least number that provided 90% of the variance accounted for was selected as the optimal number of synergies. For each subject, approximately two separate synergies and approximately six global synergies with small residual values were extracted from the separate and global electromyography datasets, respectively. Specific patterns of these muscle synergies in each task were observed during each movement. In the cross-validation method, six global synergies explained 88.0 ± 1.3% of the global dataset. These findings indicate that muscle activities underlying basic shoulder movements are expressed as six units, and these units could be proxies for shoulder muscle coordination.

Keywords

Muscle coordination; Muscle synergy; Shoulder; Electromyography

J Biomech. 2021 May 7;120:110358
doi: 10.1016/j.jbiomech.2021.110358

1. Introduction

In humans, an individual muscle seldom works independently to effectuate a joint movement. Instead, many individual muscles work together in an integrated manner to generate a net force, thereby resulting in specific joint movements (Crowninshield and Brand, 1981, Han et al., 2019). Thus, optimal coordination of several muscles involved in identical joint movements is inevitable (Dul et al., 1984, Herzog and Leonard, 1991, Hug and Tucker, 2017). Of all the joints present in humans, the shoulder joint is one of the most complex. The shoulder joint, often called the shoulder complex, consists of the glenohumeral, acromioclavicular, sternoclavicular, and scapulothoracic joints, and is surrounded by a large number of muscles (Culham and Peat, 1993, Veeger and van der Helm, 2007). Many individual muscles around the shoulder joint need to work together even when a basic shoulder movement, such as flexion or abduction, is executed.

Thus far, shoulder muscle activity measured by electromyography (EMG) has been used for the assessment of muscle coordination. Muscle activity ratio (Cools et al., 2007, Michener et al., 2016) and coactivation (Faria et al., 2009) that were calculated from the EMG amplitude within the trapezius muscle and between each part of the trapezius and the serratus anterior muscles during shoulder elevation and lowering, were proposed as indices of muscle coordination. However, the EMG amplitude is not directly related to the excitation level of the muscle during dynamic contraction (Farina, 2006) and is dependent on the normalization methods (Hug, 2011). Moreover, previous studies proposed a cross-correlation coefficient to quantify the characteristics of signal shape between two shoulder muscles (Hawkes et al., 2012a, Hawkes et al., 2012b). Nevertheless, the cross-correlation could investigate the coordination only between two muscles. Taking into account the characteristics of signal shape and a large number of muscles, an alternative index of shoulder muscle coordination is needed.

Dimensionality reduction techniques have been used to quantify the muscle coordination among numerous muscles in daily activities such as walking (Ivanenko et al., 2004, Neptune et al., 2009), running (Cappellini et al., 2006), and reaching tasks (d'Avella et al., 2006). The dimensionality reduction technique can simplify complicated muscle activations into a small number of building blocks based on the characteristics of signal shape, often called muscle synergy (d'Avella and Bizzi, 2005, Torres-Oviedo and Ting, 2007). Notably, muscle synergy can express many different patterns of muscle activity in an integrated fashion. Consequently, muscle synergy is a promising index to quantify muscle coordination when numerous EMG recordings are conducted. Nevertheless, the concern about the origin and the role of muscle synergy in terms of neurophysiology is still debatable (Bizzi and Cheung, 2013).

To our knowledge, no studies have utilized muscle synergy to comprehend muscle coordination among different shoulder muscles. The purpose of this study was to investigate muscle coordination among distinct shoulder muscles underlying basic shoulder movements based on muscle synergy. Previous studies used the dimensionality reduction technique for a separate dataset (i.e., data including single joint movement and force exertion in one direction) and global dataset (i.e., data including multi-joint movement and force exertion in multiple directions) in order to extract muscle synergy (Hagio and Kouzaki, 2014, Muceli et al., 2010). Taking the utility of the dimensionality reduction technique into account, we conducted muscle synergy extraction from both separate and global EMG datasets, including a large number of shoulder muscle activities during basic shoulder movements. We hypothesized that six or fewer muscle synergies could be extracted from both separate and global EMG datasets with less than

J Biomech. 2021 May 7;120:110358
doi: 10.1016/j.jbiomech.2021.110358

10% residuals. If this hypothesis is supported, muscle synergy could be useful to understand muscle coordination underlying basic shoulder movement.

2. Materials and methods

2.1. Participants

Thirteen men (age, 25.4 ± 3.0 years; height, 172.4 ± 4.4 cm; mass, 66.3 ± 7.0 kg) participated in the current study. The dominant arm of each subject was evaluated, and twelve subjects were identified as right-hand dominant while one was left-hand dominant. The subjects were randomly recruited from students in our institution, and the sample size was decided based on a previous study (Hug et al., 2011). None of the subjects reported a history of orthopedic, neuromuscular disorders, or pain in their dominant upper limb. All subjects provided written informed consent after explanation of all the experimental procedures, risks, and benefits associated with participation in the current study. The study design was approved by the Kyoto University Graduate School and the Faculty of Medicine Ethics Committee (R1347).

2.2. Experimental protocol

Fourteen specific shoulder movements were performed by the subjects' dominant upper limb in a custom-made space with targets set at the starting and ending positions. The custom-made space constituted of partitions, and cross-points were set as the targets indicating the starting and ending positions. The target was scaled with the shoulder range of motion of each participant, which consequently constrained their shoulder movements. In summary, five movements were associated with elevation and lowering, five were associated with horizontal abduction and adduction, and four involved rotations at different positions. For movements of elevation and lowering, the subjects raised their upper limb from the side of their body to the maximum elevation in one second and then lowered it to the starting position in one second in each of the following planes of elevation: 120° (Ele120), 90° (Ele90), 45° (Ele45), 0° (Ele0), and 30° (Ele-30) (Fig. 1A). For movements of horizontal abduction and adduction, the subjects horizontally abducted their upper limb in one second and then horizontally adducted in one second at various levels of arm elevation with each movement beginning at the plane of elevation of 90° (i.e., sagittal plane) and ending at the plane of elevation of 0° (i.e., sagittal plane). The various levels of arm elevation were as follows: 90° (Hor0), 120° (Hor30), 150° (Hor60), 60° (Hor-30), and 30° (Hor-60) (Fig. 1B). For movements of rotation, the subjects maximally rotated their shoulder joint (i.e., the humerothoracic joint) from the maximal internal rotation to the maximal external rotation with the upper limb placed on the side of the body (Rot1), at 90° abduction (Rot2), 90° flexion (Rot3), and maximal elevation (Rot4) (Fig. 1C). Each movement was ordered randomly and repeated twelve times with suitable intervals to prevent fatigue. During all of the movements, the subjects were asked to keep their face and trunk straight and their elbow joint fully extended and to reduce the movement of the forearm, hand, and fingers as much as possible. The movement speed of each movement was maintained at 60 beats per minute using a metronome. The subjects underwent sufficient practice for each movement. A wireless accelerometer (DTS; Noraxon, Scottsdale, AZ, USA) was placed on the back of the subjects' hand, and the acceleration of the upper limb during the performance of the shoulder movements was measured at a

J Biomech. 2021 May 7;120:110358
doi: 10.1016/j.jbiomech.2021.110358

sampling rate of 1500 Hz. The measured acceleration was used to identify the start and end of the shoulder movements.

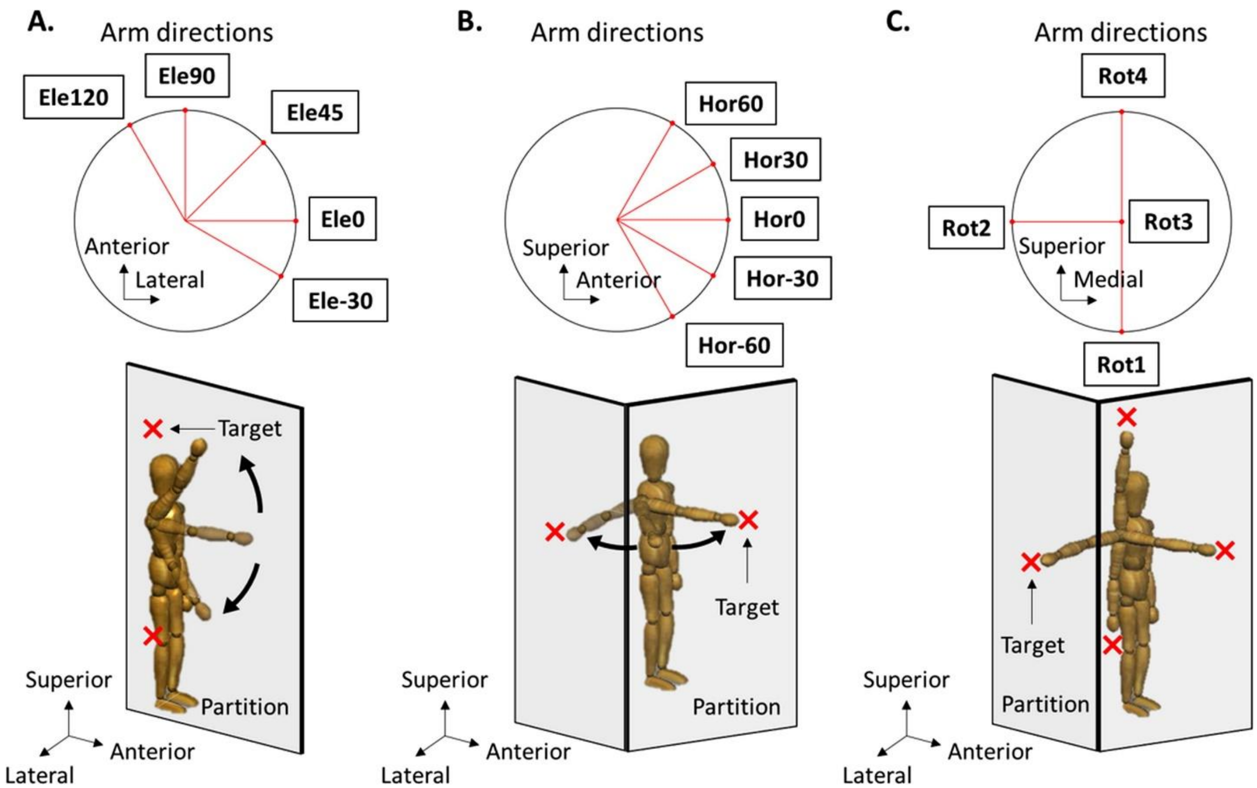

Fig. 1. Experimental setup and arm directions. The participants performed shoulder movements in a custom-made space guided by the cross-shaped targets on the partitions. Elevation and lowering movements (Panel A), horizontal abduction and adduction movements (Panel B), and rotation movements (Panel C). The circles represent the arm directions for basic shoulder movements. The centroid and red lines in each circle represent the center of the shoulder joint and arm directions, respectively, from a given points of view during the shoulder movements. (For interpretation of the references to color in this figure legend, the reader is referred to the web version of this article.)

2.3. Surface electromyography

Muscle activity was measured from 12 muscle portions using surface electromyography (EMG) (TeleMyo DTS; Noraxon, Scottsdale, AZ, USA), amplified (common mode rejection ratio > 100 dB; input impedance > 100 Mohm; gain 500 dB), and digitized at a sampling rate of 1500 Hz. The skin area for the placement of the electrodes was shaved and cleaned by scrubbing and alcohol. Disposable pregelled Ag-AgCl electrodes (Blue Sensor; Medicotest, Olstykke, Denmark) were placed on the following 12 muscle portions in the upper limb and trunk of the dominant side: anterior, middle, and posterior deltoid (AD, MD, PD), upper,

J Biomech. 2021 May 7;120:110358
doi: 10.1016/j.jbiomech.2021.110358

middle, and lower trapezius (UT, MT, LT), infraspinatus (ISP), latissimus dorsi (LD), biceps brachii (BB), long head of triceps brachii (TB), serratus anterior (SA), and pectoralis major (PM) in accordance with Surface Electromyography for Non-Invasive Assessment of Muscle (SENIAM) guidelines (http://www.seniam.org/) and previous studies (Cools et al., 2007, de Seze and Cazalets, 2008, Ekstrom et al., 2004, Jaggi et al., 2009, Kibler et al., 2008). All electrode placements and their references are summarized in Table 1. The inter-electrode distance was kept at 20 mm as per the SENIAM recommendation.

Table 1. Electrode placements for each muscle and its portion

Muscles	Sites	References
Anterior deltoid (AD)	One finger width distal and anterior to scapular acromion	Kibler et al., 2008
Middle deltoid (MD)	Greatest bulge of the muscle on the line from the scapular acromion to the lateral epicondyle of the elbow	Cools et al., 2007
Posterior deltoid (PD)	2cm below posterior crista of the scapular acromion	Kibler et al., 2008
Upper trapezius (UT)	Middle point between the spinous process of the seventh cervical vertebra and scapular acromion	Cools et al., 2007
Middle trapezius (MT)	Middle point on the horizontal line between the root of the scapular spine and third thoracic spine	Cools et al., 2007
Lower trapezius (LT)	Middle point between the spinous process of the seventh cervical vertebra and the trigonum scapula	Cools et al., 2007
Infraspinatus (ISP)	Halfway point between the inferior angle of the scapula and the middle point between the acromion and the trigonum scapula	Jaggi et al., 2009
Latissimus dorsi (LD)	Muscular curve at the 12th thoracic vertebra and along the line connecting the most posterior point of the posterior axillary fold and second sacrum spinous process	de Sèze and Cazalets, 2008
Biceps brachii (BB)	Line between the medial acromion and fossa cubit at one-third point from the fossa cubit.	SENIAM guidelines
Long head of triceps brachii (TB)	Middle point between the posterior crista of the scapular acromion and	SENIAM guidelines

J Biomech. 2021 May 7;120:110358
doi: 10.1016/j.jbiomech.2021.110358

	olecranon at two finger widths medial to the line	
Serratus anterior (SA)	Middle point between the leading edge of the latissimus dorsi and the trailing edge of the pectoralis major on the seventh rib	Ekstrom et al., 2004
Pectoralis major (PM)	3cm below the one-third line from the medial clavicular head to the scapular acromion	Jaggi et al., 2009

SENIAM: Surface Electromyography for Non-Invasive Assessment of Muscle (http://www.seniam.org/)

2.4. Data processing

The measured raw EMG signals were high-pass filtered at 20 Hz (De Luca et al., 2010) using a zero-phase-lag fourth-order Butterworth filter and rectified. The rectified EMG signals were then low-pass filtered at 4 Hz (Clark et al., 2010) using a zero-phase-lag fourth-order Butterworth filter to make EMG envelopes. The EMG envelopes were normalized by the maximal value of each muscle in all movements. According to the measured acceleration during the shoulder movements, the start and end of each trial was identified. Ten trials, except the first and last trials, were used for further analysis. The muscle activities for maintaining the start and end postures of the upper limb were excluded in each trial using a subtraction procedure described in a previous study (d'Avella et al., 2006), in order to focus on the component of the muscle pattern associated with upper limb movement. When negative activity occurred by the subtraction procedure, we assumed the negative activity as the zero value for further dimensionality reduction technique described in muscle synergy extraction. This procedure was used for ten trials. The EMG signals were downsampled; consequently, 3000 data points were compressed into 100 timepoints in each trial.

2.5. Muscle synergy extraction

Muscle synergies as the index of muscle coordination were extracted in two different ways for individual subjects to verify their utility for various types of movement. The muscle synergy extraction from separate EMG datasets consisting of 12 muscle portions × 1000 bins (100 timepoints × 10 trials) was called separate muscle synergy, while the the extraction from global EMG datasets consisting of 12 muscle regions × 14,000 bins (14 movements × 100 timepoints × 10 trials) was called global muscle synergy.

For muscle synergy extraction, the processed EMG signals in the global and separate EMG datasets were scaled to have unit variance (Sawers et al., 2015, Torres-Oviedo et al., 2006). Unit variance scaling was applied to avoid large representations of high-variance muscles in output synergy weightings (Cheung et al., 2009). Non-negative matrix factorization (NMF), referred to as the dimensionality reduction technique (Lee and Seung, 1999) was used to extract muscle synergies from global and separate EMG datasets. NMF assumes that the muscle activation pattern (E) is composed of a linear combination of the muscle

J Biomech. 2021 May 7;120:110358
doi: 10.1016/j.jbiomech.2021.110358

weighting (W) and the activation coefficient (C) of muscle synergy. Therefore, the muscle activation pattern for each movement is represented via the following equation (1):

$$\mathrm{E} = \mathrm{WC} + \mathrm{e}\ (\mathrm{W} \geq 0, \mathrm{C} \geq 0) \qquad (1)$$

where E is a p × n matrix (where p is the number of muscle portions and n is the number of timepoints), W is a p × k matrix of the weighting vector representing the spatial component, C is a k × n matrix of the activation coefficient representing the temporal component, k is the number of extracted synergies, and e is the residual. After extraction of the muscle synergies, the variance of the muscle weighting returned. This technique was repeated 20 times, in accordance with a previous study (Cheung et al., 2005). Note that we extracted the muscle synergies using NMF in Matlab (Statistics and Machine Learning Toolbox, MathWorks, Inc., Natick, Massachusetts, United States).

We iterated the analysis by varying the number of muscle synergies from 1 to 12 to identify the optimal number of muscle synergies to sufficiently reconstruct the dataset. Then goodness-of-fit was calculated as the variance accounted for (VAF) between the measured and reconstructed datasets to identify the optimal number of synergies using the following equation (2):

$$\mathrm{VAF} = \left(1 - \frac{\sum_{i=1}^{p}\sum_{j=1}^{n}\left(e_{i,j}\right)^2}{\sum_{i=1}^{p}\sum_{j=1}^{n}\left(E_{i,j}\right)^2}\right) \times 100 \qquad (2)$$

We defined the least number that provided 90% of the VAF as the optimal number of synergies in each dataset (Torres-Oviedo et al., 2006).

2.6. Functional sorting of global synergy

To confirm whether the global synergies were similar across subjects, we performed functional sorting. The classification was performed by grouping the muscle weighting of the global synergy based on cosine similarity with arbitrary subjects using an iterative process. Then, we averaged the functionally sorted muscle weighting across all subjects and further calculated the cosine similarity between the averaged muscle weighting and that of each subject (Torres-Oviedo and Ting, 2007). If two synergies were classified into the same synergy group in one subject, we defined the pair of synergies with the highest correlation as the same group of synergies in accordance with the previous study (Hagio and Kouzaki, 2014).

2.7. Validation of extracted muscle synergy

The cross-validation method was used to verify the robustness of the muscle synergy extracted from the global dataset for each subject (Cheung et al., 2005). The data for each movement in the global dataset were divided into four equal partitions. One of the four partitions was randomly defined as a training dataset, while three were defined as test datasets. Muscle synergies were extracted from these datasets. In order to update the muscle weighting and activation coefficient of the test dataset, the activation coefficient was updated, whereas the muscle weighting was fixed by that of the training dataset. This

J Biomech. 2021 May 7;120:110358
doi: 10.1016/j.jbiomech.2021.110358

cross-validation process was iterated 20 times using different weightings and activations due to changes in the divided partition of the dataset. The goodness-of-fit was assessed using the VAF.

Additionally, we calculated the VAF from the shuffled global dataset with the 20 iterations process for each subject. For this shuffling process, the data of each muscle were independently shuffled, so that the temporal order of each muscle activity was removed, whereas the value, range, and variance were maintained (Chvatal et al., 2011).

3. Results

3.1. Muscle activities

Muscle activities were measured from 12 muscle portions during 14 shoulder movements using a surface EMG, and the EMG envelopes were then calculated. Fig. 2 shows all of the EMG envelopes in a representative subject. As a feature of these EMG envelopes, some measured muscles were recruited and activated in each movement, and the pattern and peak of the muscle activity tended to be different across muscles for a given motion.

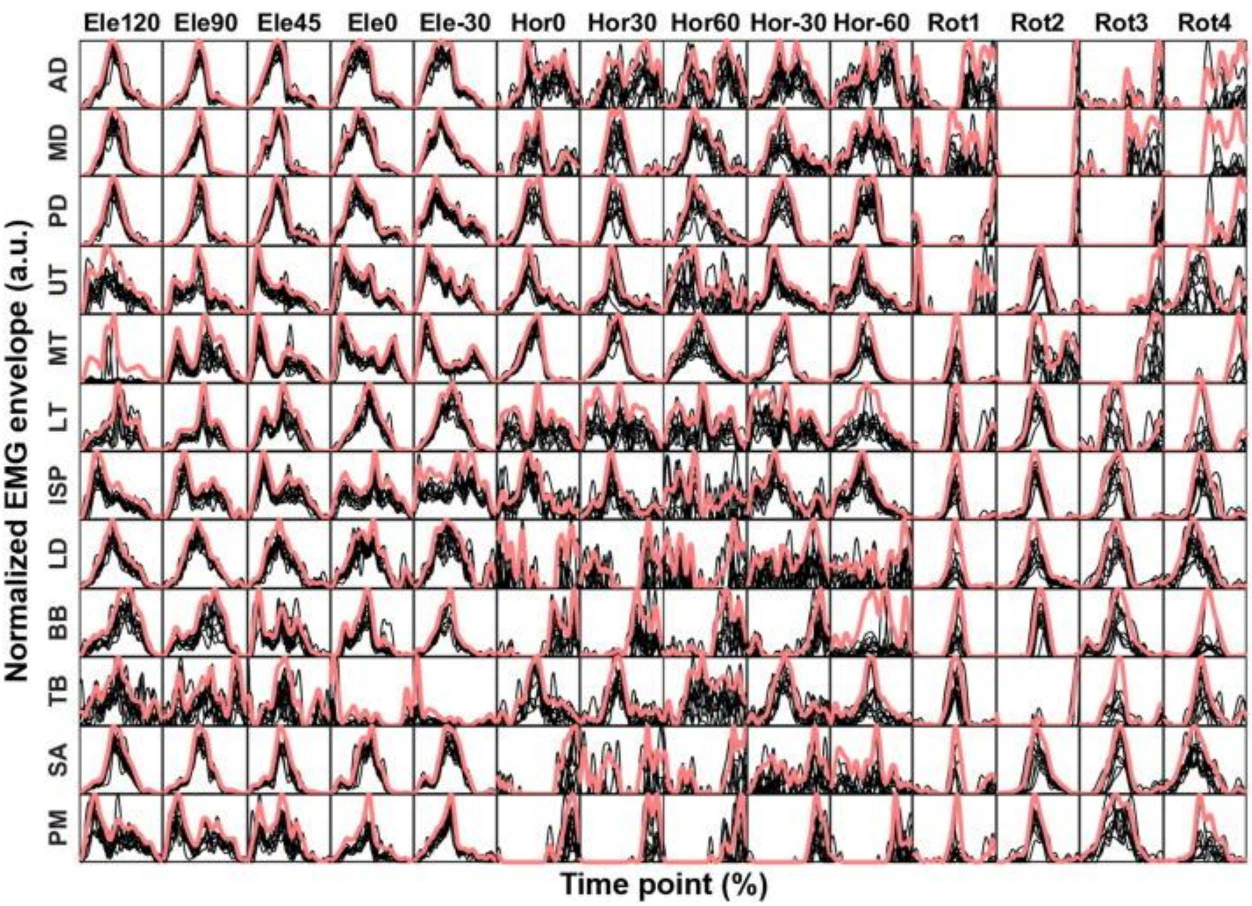

Fig. 2. Electromyographic (EMG) envelopes of 12 muscle portions measured in each basic shoulder movement for a representative subject. Black lines are the EMG envelopes of 10 trials in each shoulder

J Biomech. 2021 May 7;120:110358
doi: 10.1016/j.jbiomech.2021.110358

movement. Red line is the mean value of all EMG envelope. The both EMG envelopes were normalized by the maximal value of each muscle in each movement to easily compare each other muscles.

3.2. Global and separate synergies

The VAFs for global synergy representing the goodness-of-fit for the calculation of the muscle synergy in each subject are shown in Fig. 3. According to the criterion used to extract the optimal number of muscle synergies, 5–7 global synergies extracted from the global dataset across the subjects (5: 7.6%, 6: 76.9%, 7: 15.3%), and the mean number of global synergies was 6.0 ± 0.4. Fig. 4 shows global synergies in a representative subject. The VAFs for separate synergies are shown in Fig. 5. Separate synergies accounted for the separate datasets across the movements (Ele120: 2.3 ± 0.4, Ele90: 2.5 ± 0.6, Ele45: 2.3 ± 0.4, Ele0: 2.3 ± 0.4, Ele-30: 2.0 ± 0.7, Hor0: 3.2 ± 0.9, Hor30: 3.1 ± 0.7, Hor60: 3.0 ± 1.1, Hor-30: 2.9 ± 0.7, Hor-60: 3.0 ± 1.2, Rot1: 1.5 ± 0.5, Rot2: 2.5 ± 0.7, Rot3: 2.3 ± 0.9, Rot4: 2.9 ± 0.8), and the mean number of separate synergies was 2.6 ± 0.9. The weighting vectors and the profiles of activation coefficients of the separate synergies are shown in Fig. 6. Note that the number of separate and global synergies and the weighting vectors of each muscle rarely changed even when unit variance scaling was not applied.

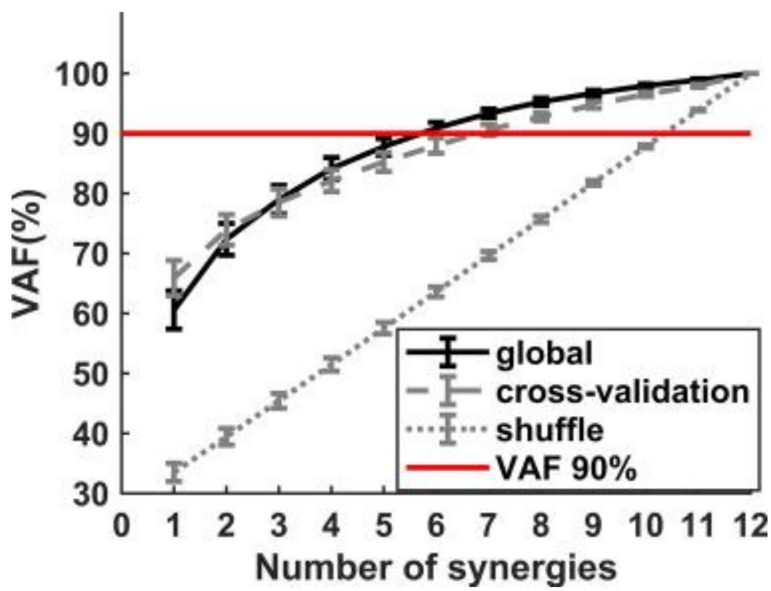

Fig. 3. Averaged variance accounted for (VAF) to determined optimal number of global muscle synergy in all subjects. The black solid line represents the VAF for determination of global synergy. The gray dashed lines and dotted line represent the VAF calculated from cross-validation method and shuffled dataset respectively. The error bars are standard deviation across subjects. The horizontal red line indicates the VAF 90%, meaning the threshold to determined optimal number of global muscle synergy.

J Biomech. 2021 May 7;120:110358
doi: 10.1016/j.jbiomech.2021.110358

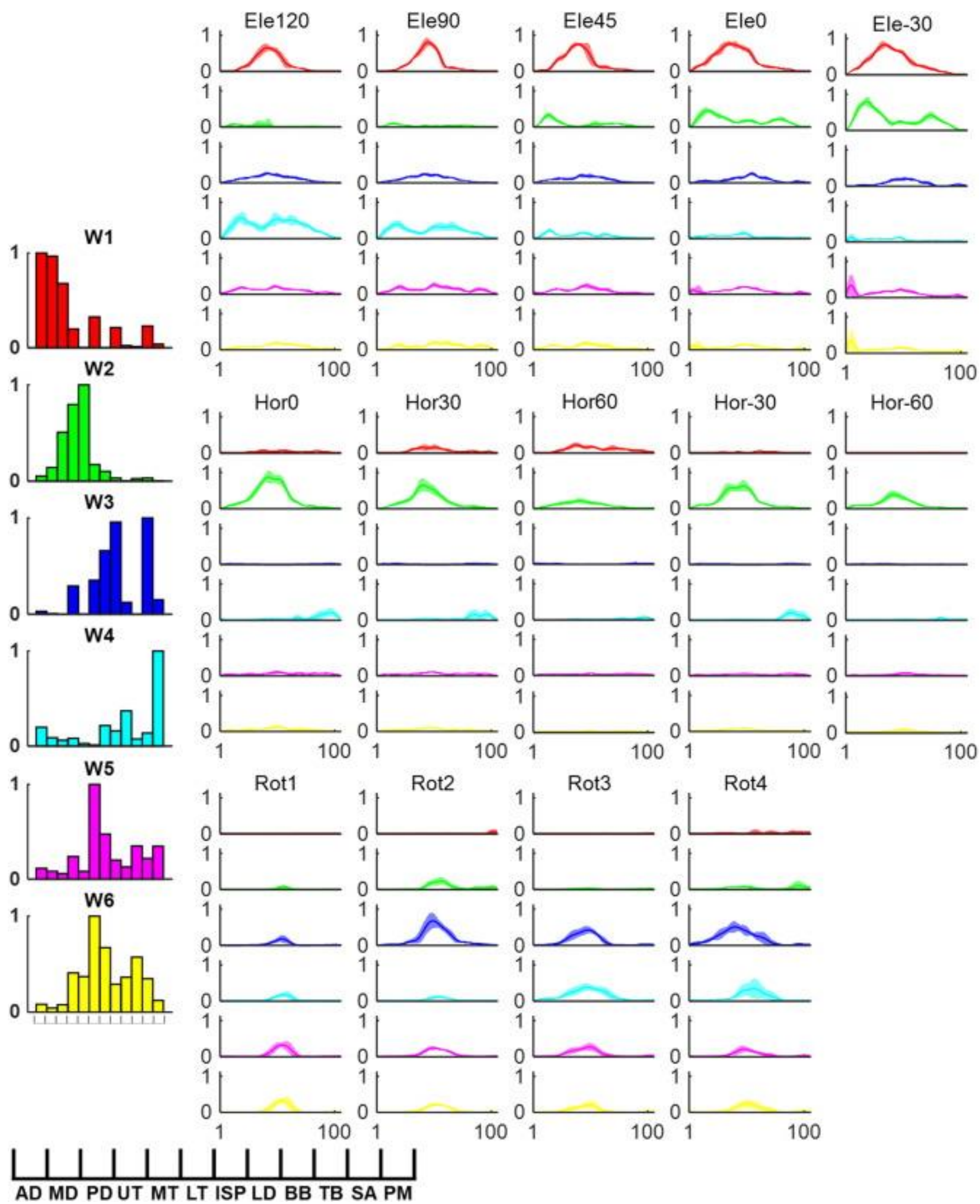

Fig. 4. Global synergy across all basic shoulder movements for a representative subject. Bars and lines with shaded area represent muscle weighing and activation coefficient respectively. The line and shaded area for activation coefficient are the mean value and standard deviation across the 10 trials respectively. Each color means functional sorted global synergy from 1 to 6. W represents the number of global synergies.

J Biomech. 2021 May 7;120:110358
doi: 10.1016/j.jbiomech.2021.110358

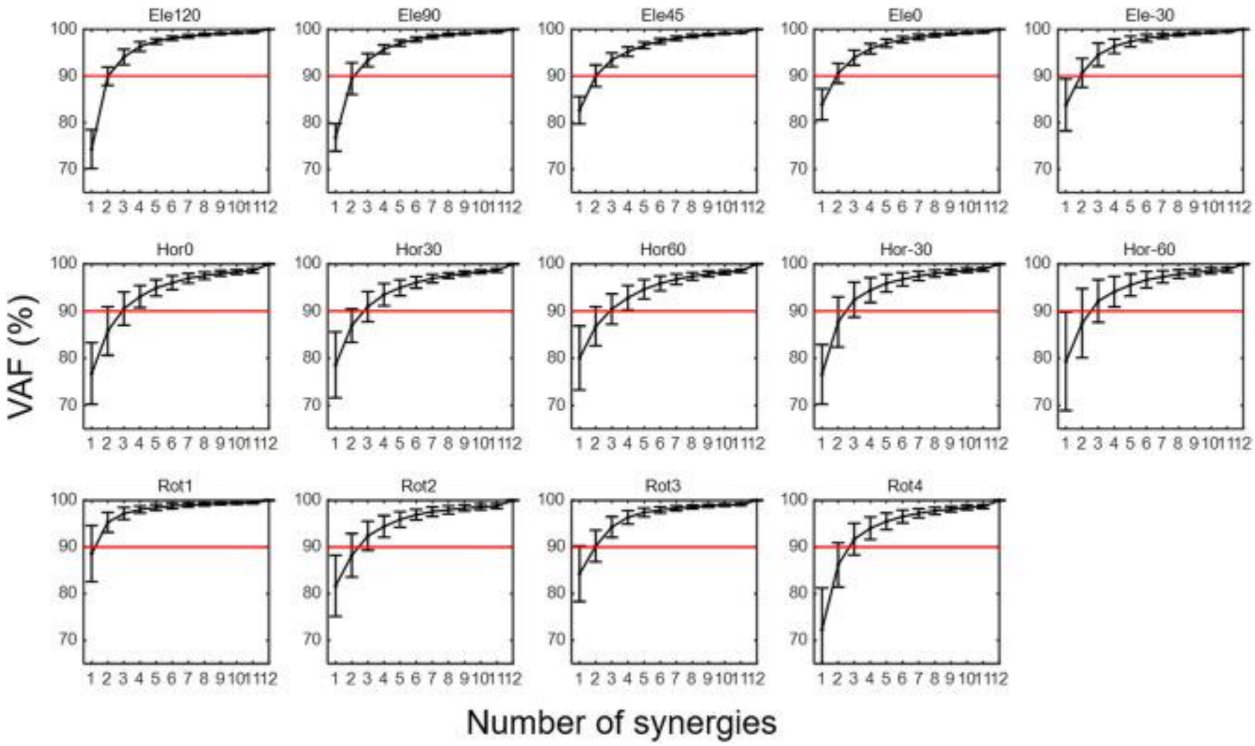

Fig. 5. Averaged variance accounted for (VAF) to determined optimal number of separate muscle synergy in all basic shoulder movements. The black solid line represents the VAF for determination of separate synergy. The horizontal red lines indicate the VAF 90%, meaning the threshold to determined optimal number of separate muscle synergy.

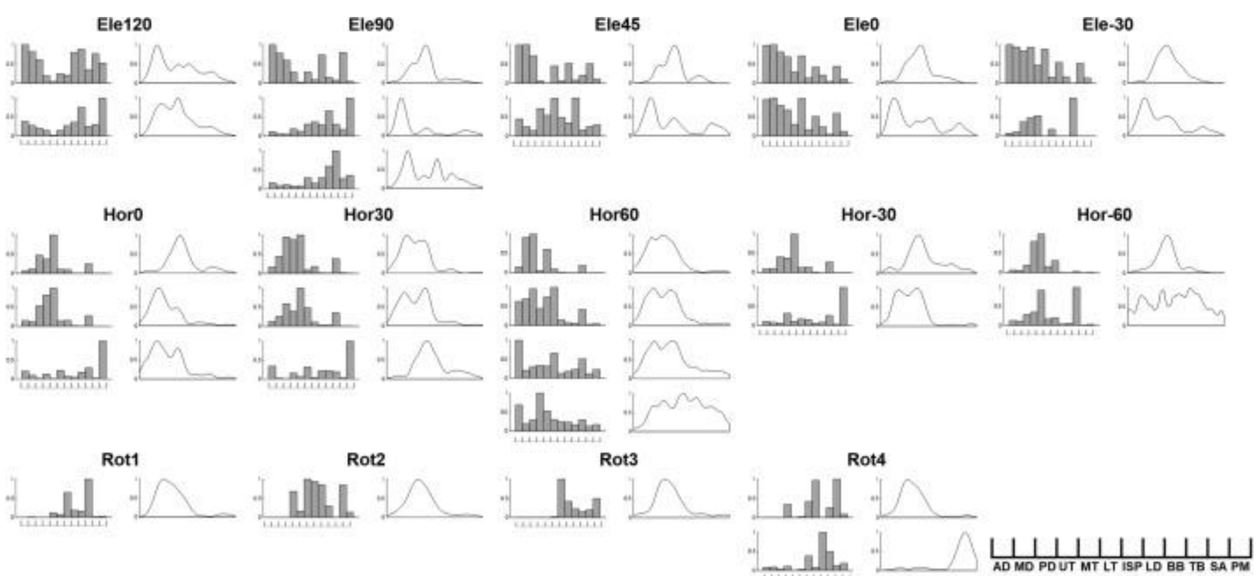

Fig. 6. Separate synergy across all basic shoulder movements for a representative subject. Bars and lines represent muscle weighing and activation coefficient respectively.

J Biomech. 2021 May 7;120:110358
doi: 10.1016/j.jbiomech.2021.110358

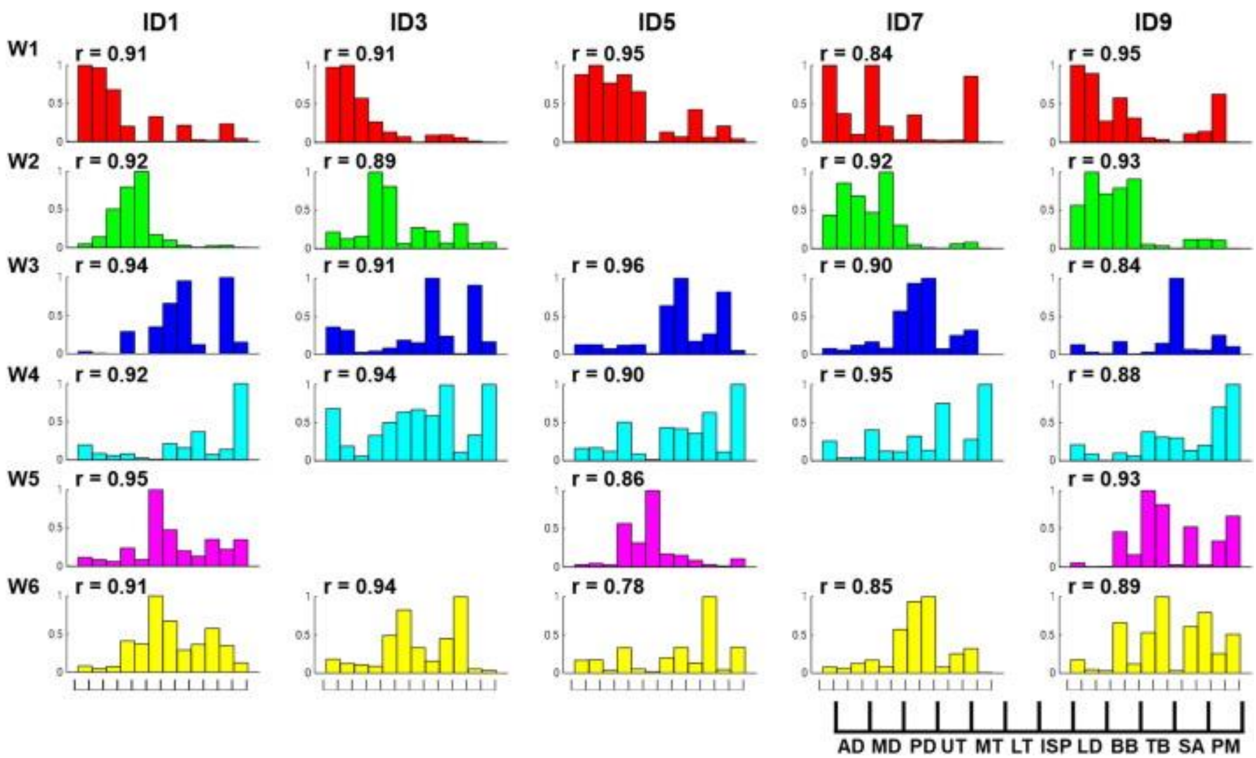

Fig. 7. Muscle weighting of global synergies for representative subjects. The r values represent cosine similarities between the averaged global synergy calculated from functional sorting and the global synergy in each subject. W represents the number of global synergies from 1 to 6. ID represents the identification number subjects of 1, 3, 5, 7, and 9.

Using functional sorting of the global synergies, the extracted global synergies were categorized into six global synergies. The cosine similarities between the averaged global synergy across the subjects and the global synergy in each subject ranged from 0.78 to 0.97. Fig. 7 depicts the functionally sorted global synergies; notabley, muscles with high weighting vector work coordinately during shoulder movements as a functional unit. For the weighting of each muscle synergy, synergy 1 consisted of AD, MD, and UT, and was activated in the elevation phase of the movements associated with elevation and lowering. Synergy 2 showed a large weighting of PD, UT, and MT, and a large activation coefficient in the horizontal abduction phase of the movements associated with horizontal abduction and adduction. Synergy 3 and 6 dominated the weighting of ISP, LD, and SA, and that of ISP and TB, respectively, and were activated during changes in the internal and external rotations. Synergy 4, weighted by PM, was activated in a wide range of movements associated with elevation and lowering, in the horizontal adduction phase of the movements associated with horizontal abduction and adduction, and at the point of change in the internal and external rotations. Synergy 5 showed a large weighting of LT and ISP and the activation coefficient in a wide range of movements associated with elevation and lowering and at the point of change in the internal and external rotations.

J Biomech. 2021 May 7;120:110358
doi: 10.1016/j.jbiomech.2021.110358

3.3. Validation of muscle synergy extraction

The VAFs for the muscle synergies extracted from the cross-validation method and shuffled dataset are shown in Fig. 3. The VAFs calculated from the global dataset and the cross-validation method seemed to be similar, although the VAF calculated from the shuffled dataset is less than that calculated from the global dataset.

4. Discussion

The present study extracted muscle synergies from the muscle activities of 12 shoulder muscle portions measured by surface EMG during basic shoulder movements. The results showed that around two separate synergies were extracted from the separate EMG dataset and around six global synergies were extracted from the global EMG dataset across the subjects according to the criteria defined as 90% of VAF. These results supported our hypothesis that six or fewer muscle synergies could be extracted from both separate and global EMG datasets with less than 10% residuals. To our knowledge, this is the first study to clarify muscle coordination among different shoulder muscles underlying basic shoulder movements from the perspective of muscle synergy.

Around two separate synergies were extracted from separate EMG datasets across movements in each subject. A previous study showed that two synergies were sufficient for explaining single joint movements such as elbow flexion and extension, and suggested that one synergy contributes to either flexion or extension (Muceli et al., 2010). Our results are concordant with those of that study, and suggest that muscle synergies represent muscle coordination dependent on any given shoulder movement.

Around six global synergies were extracted from the global EMG dataset across subjects and were categorized into six groups based on the results of functional sorting. Previous studies found three to five muscle synergies during multidirectional reaching (d'Avella et al., 2008, d'Avella et al., 2006), three muscle synergies during grasping tasks (Overduin et al., 2008), and 3–5 muscle synergies during three-dimensional force generation (Roh et al., 2012). The extracted muscle synergy was affected by biomechanical and task constraints (Kutch and Valero-Cuevas, 2012, Todorov, 2004), the number and choice of muscles (Steele et al., 2013), and the criteria for the number of muscle synergies (i.e., VAF, R2, and z-score based VAF) (Banks et al., 2017, Shuman et al., 2017). Although it is difficult to directly compare the component of the muscle synergies in previous studies with that of the current study from the point of view of methodology, the set of 14 movements as basic shoulder movement is likely to be a reasonable movement sample set that represents the entire movement repertoire available around the shoulder joint because these movements demand a large range of motion and multiplanar actions within the shoulder joint. Therefore, the global synergy extracted from the concatenated EMG dataset could be a unit of muscle coordination for basic shoulder movements.

Muscle weighting could be meaningful for the muscle coordination among the shoulder muscles and indicate that the muscles with large muscle weighting work in close coordination. For instance, the muscle weightings of AD, MD, LD, and SA were relatively large in separate synergy 1 of the movement of Ele90, which means that these muscles with large muscle weighting coordinately work in the Flex. Moreover, global synergy 1 possessed relatively large muscle weighting of AD, MD, and UT, which implies that these

J Biomech. 2021 May 7;120:110358
doi: 10.1016/j.jbiomech.2021.110358

muscles coordinately work through the basic shoulder movement because the EMG dataset extracted the global synergy consisting of shoulder muscle activities during all movements.

In a clinical setting, alteration of muscle synergy has been observed not only in patients with brain damage, such as stroke (Cheung et al., 2012) and cerebral palsy (Tang et al., 2015), but also in those with musculoskeletal disorders such as femoroacetabular impingement (Diamond et al., 2017) and gluteal tendinopathy (Allison et al., 2018). Additionally, through the process of motor learning, the number and/or components of muscle synergies have been modified in humans (Asaka et al., 2008, Danna-Dos-Santos et al., 2008) and animals (Kargo and Nitz, 2003). Taken together, focus on patient-specific muscle synergies in shoulder disorders and understanding the change in movement due to modification of the muscle synergies may be of therapeutic interest in shoulder rehabilitation strategies.

The current study, however, has some limitations. First, a comparison of the activation coefficient in muscle synergy among the different shoulder movements was not performed. To achieve our purpose, we set the shoulder multiplanar movement as much as possible, resulting in a different range of motion among the shoulder movements. Due to this methodology, comparison of the activation coefficient among the shoulder movements was difficult. Further, studies to investigate not only the spatial component but also the temporal component in muscle synergies are needed. Second, the maintenance of a constant speed of motion without an isokinetic machine is not possible. The current study, however, had a sufficiently extended familiarization session before the actual measurement and used a metronome during experimentation. Additionally, previous studies identified a transition of the activation coefficient with gait speed and few changes in muscle weighting (Cappellini et al., 2006, Ivanenko et al., 2004). Therefore, shoulder movement speed seldom affects the component of muscle synergy that we focused upon. Third, some potential drawbacks of surface EMG, such as the inability to measure deep muscle activity, signal interference due to crosstalk of surrounding muscles, and the change in monitored motor units due to the sliding of muscle with motion beneath the electrode sites were unavoidable. Deep muscles such as the supraspinatus and subscapularis, part of the rotator cuff muscles, play an important role in the shoulder joint (Codman, 1990). A determinative study that overcomes these limitations using a fine-wire EMG is warranted to comprehend shoulder muscles coordination in the context of muscle synergy.

In conclusion, we clarified around two separate and six global synergies extracted from the EMG dataset of 12 shoulder muscle portions underlying basic shoulder movements using the dimensionality reduction technique. Many shoulder muscles work in a coordinated fashion based on a small number of units during basic shoulder movements.

Declaration of Competing Interest

The authors declare that they have no known competing financial interests or personal relationships that could have appeared to influence the work reported in this paper.

Acknowledgements

The authors thank Shota Hagio (Kyoto University) for insights on the extraction methods of separate and global synergies and helping with cross-validation analysis, and Satoko Ibuki (Kyoto University) and Editage (www.editage.com) for language editing and proofreading. This work was supported by the Japan Society for the Promotion Science Research Fellow (18J12658, 20J01660).

References

Allison, K., Salomoni, S.E., Bennell, K.L., Wrigley, T.V., Hug, F., Vicenzino, B., Grimaldi, A., Hodges, P.W., 2018. Hip abductor muscle activity during walking in individuals with gluteal tendinopathy. Scand J Med Sci Sports 28, 686-695.

Asaka, T., Wang, Y., Fukushima, J., Latash, M.L., 2008. Learning effects on muscle modes and multi-mode postural synergies. Exp Brain Res 184, 323-338.

Banks, C.L., Pai, M.M., McGuirk, T.E., Fregly, B.J., Patten, C., 2017. Methodological Choices in Muscle Synergy Analysis Impact Differentiation of Physiological Characteristics Following Stroke. Front Comput Neurosci 11, 78.

Bizzi, E., Cheung, V.C., 2013. The neural origin of muscle synergies. Front Comput Neurosci 7, 51.

Cappellini, G., Ivanenko, Y.P., Poppele, R.E., Lacquaniti, F., 2006. Motor patterns in human walking and running. J Neurophysiol 95, 3426-3437.

Cheung, V.C., d'Avella, A., Bizzi, E., 2009. Adjustments of motor pattern for load compensation via modulated activations of muscle synergies during natural behaviors. J Neurophysiol 101, 1235-1257.

Cheung, V.C., d'Avella, A., Tresch, M.C., Bizzi, E., 2005. Central and sensory contributions to the activation and organization of muscle synergies during natural motor behaviors. J Neurosci 25, 6419-6434.

Cheung, V.C., Turolla, A., Agostini, M., Silvoni, S., Bennis, C., Kasi, P., Paganoni, S., Bonato, P., Bizzi, E., 2012. Muscle synergy patterns as physiological markers of motor cortical damage. Proc Natl Acad Sci U S A 109, 14652-14656.

Chvatal, S.A., Torres-Oviedo, G., Safavynia, S.A., Ting, L.H., 2011. Common muscle synergies for control of center of mass and force in nonstepping and stepping postural behaviors. J Neurophysiol 106, 999-1015.

Clark, D.J., Ting, L.H., Zajac, F.E., Neptune, R.R., Kautz, S.A., 2010. Merging of healthy motor modules predicts reduced locomotor performance and muscle coordination complexity post-stroke. J Neurophysiol 103, 844-857.

Codman, E.A., 1990. Rupture of the supraspinatus tendon. 1911. Clin Orthop Relat Res, 3-26.

Cools, A.M., Declercq, G.A., Cambier, D.C., Mahieu, N.N., Witvrouw, E.E., 2007. Trapezius activity and intramuscular balance during isokinetic exercise in overhead athletes with impingement symptoms. Scand J Med Sci Sports 17, 25-33.

Crowninshield, R.D., Brand, R.A., 1981. The prediction of forces in joint structures; distribution of intersegmental resultants. Exerc Sport Sci Rev 9, 159-181.

J Biomech. 2021 May 7;120:110358
doi: 10.1016/j.jbiomech.2021.110358

Culham, E., Peat, M., 1993. Functional anatomy of the shoulder complex. J Orthop Sports Phys Ther 18, 342-350.

d'Avella, A., Bizzi, E., 2005. Shared and specific muscle synergies in natural motor behaviors. Proc Natl Acad Sci U S A 102, 3076-3081.

d'Avella, A., Fernandez, L., Portone, A., Lacquaniti, F., 2008. Modulation of phasic and tonic muscle synergies with reaching direction and speed. J Neurophysiol 100, 1433-1454.

d'Avella, A., Portone, A., Fernandez, L., Lacquaniti, F., 2006. Control of fast-reaching movements by muscle synergy combinations. J Neurosci 26, 7791-7810.

Danna-Dos-Santos, A., Degani, A.M., Latash, M.L., 2008. Flexible muscle modes and synergies in challenging whole-body tasks. Exp Brain Res 189, 171-187.

De Luca, C.J., Gilmore, L.D., Kuznetsov, M., Roy, S.H., 2010. Filtering the surface EMG signal: Movement artifact and baseline noise contamination. J Biomech 43, 1573-1579.

de Seze, M.P., Cazalets, J.R., 2008. Anatomical optimization of skin electrode placement to record electromyographic activity of erector spinae muscles. Surg Radiol Anat 30, 137-143.

Diamond, L.E., Van den Hoorn, W., Bennell, K.L., Wrigley, T.V., Hinman, R.S., O'Donnell, J., Hodges, P.W., 2017. Coordination of deep hip muscle activity is altered in symptomatic femoroacetabular impingement. J Orthop Res 35, 1494-1504.

Dul, J., Townsend, M.A., Shiavi, R., Johnson, G.E., 1984. Muscular synergism--I. On criteria for load sharing between synergistic muscles. J Biomech 17, 663-673.

Ekstrom, R.A., Bifulco, K.M., Lopau, C.J., Andersen, C.F., Gough, J.R., 2004. Comparing the function of the upper and lower parts of the serratus anterior muscle using surface electromyography. J Orthop Sports Phys Ther 34, 235-243.

Faria, C.D., Teixeira-Salmela, L.F., Gomes, P.F., 2009. Applicability of the coactivation method in assessing synergies of the scapular stabilizing muscles. J Shoulder Elbow Surg 18, 764-772.

Farina, D., 2006. Interpretation of the surface electromyogram in dynamic contractions. Exerc Sport Sci Rev 34, 121-127.

Hagio, S., Kouzaki, M., 2014. The flexible recruitment of muscle synergies depends on the required force-generating capability. J Neurophysiol 112, 316-327.

Han, S.W., Sawatsky, A., de Brito Fontana, H., Herzog, W., 2019. Contribution of individual quadriceps muscles to knee joint mechanics. J Exp Biol 222.

Hawkes, D.H., Alizadehkhaiyat, O., Fisher, A.C., Kemp, G.J., Roebuck, M.M., Frostick, S.P., 2012a. Normal shoulder muscular activation and co-ordination during a shoulder elevation task based on activities of daily living: an electromyographic study. J Orthop Res 30, 53-60.

Hawkes, D.H., Alizadehkhaiyat, O., Kemp, G.J., Fisher, A.C., Roebuck, M.M., Frostick, S.P., 2012b. Shoulder muscle activation and coordination in patients with a massive rotator cuff tear: an electromyographic study. J Orthop Res 30, 1140-1146.

Herzog, W., Leonard, T.R., 1991. Validation of optimization models that estimate the forces exerted by synergistic muscles. J Biomech 24 Suppl 1, 31-39.

Hug, F., 2011. Can muscle coordination be precisely studied by surface electromyography? J Electromyogr Kinesiol 21, 1-12.

Hug, F., Tucker, K., 2017. Muscle Coordination and the Development of Musculoskeletal Disorders. Exerc Sport Sci Rev 45, 201-208.

Hug, F., Turpin, N.A., Couturier, A., Dorel, S., 2011. Consistency of muscle synergies during pedaling across different mechanical constraints. J Neurophysiol 106, 91-103.

Ivanenko, Y.P., Poppele, R.E., Lacquaniti, F., 2004. Five basic muscle activation patterns account for muscle activity during human locomotion. J Physiol 556, 267-282.

Jaggi, A., Malone, A.A., Cowan, J., Lambert, S., Bayley, I., Cairns, M.C., 2009. Prospective blinded comparison of surface versus wire electromyographic analysis of muscle recruitment in shoulder instability. Physiother Res Int 14, 17-29.

Kargo, W.J., Nitz, D.A., 2003. Early skill learning is expressed through selection and tuning of cortically represented muscle synergies. J Neurosci 23, 11255-11269.

Kibler, W.B., Sciascia, A.D., Uhl, T.L., Tambay, N., Cunningham, T., 2008. Electromyographic analysis of specific exercises for scapular control in early phases of shoulder rehabilitation. Am J Sports Med 36, 1789-1798.

Kutch, J.J., Valero-Cuevas, F.J., 2012. Challenges and new approaches to proving the existence of muscle synergies of neural origin. PLoS Comput Biol 8, e1002434.

Lee, D.D., Seung, H.S., 1999. Learning the parts of objects by non-negative matrix factorization. Nature 401, 788-791.

Michener, L.A., Sharma, S., Cools, A.M., Timmons, M.K., 2016. Relative scapular muscle activity ratios are altered in subacromial pain syndrome. J Shoulder Elbow Surg 25, 1861-1867.

Muceli, S., Boye, A.T., d'Avella, A., Farina, D., 2010. Identifying representative synergy matrices for describing muscular activation patterns during multidirectional reaching in the horizontal plane. J Neurophysiol 103, 1532-1542.

Neptune, R.R., Clark, D.J., Kautz, S.A., 2009. Modular control of human walking: a simulation study. J Biomech 42, 1282-1287.

Overduin, S.A., d'Avella, A., Roh, J., Bizzi, E., 2008. Modulation of muscle synergy recruitment in primate grasping. J Neurosci 28, 880-892.

Roh, J., Rymer, W.Z., Beer, R.F., 2012. Robustness of muscle synergies underlying three-dimensional force generation at the hand in healthy humans. J Neurophysiol 107, 2123-2142.

Sawers, A., Allen, J.L., Ting, L.H., 2015. Long-term training modifies the modular structure and organization of walking balance control. J Neurophysiol 114, 3359-3373.

J Biomech. 2021 May 7;120:110358
doi: 10.1016/j.jbiomech.2021.110358

Shuman, B.R., Schwartz, M.H., Steele, K.M., 2017. Electromyography Data Processing Impacts Muscle Synergies during Gait for Unimpaired Children and Children with Cerebral Palsy. Front Comput Neurosci 11, 50.

Steele, K.M., Tresch, M.C., Perreault, E.J., 2013. The number and choice of muscles impact the results of muscle synergy analyses. Front Comput Neurosci 7, 105.

Tang, L., Li, F., Cao, S., Zhang, X., Wu, D., Chen, X., 2015. Muscle synergy analysis in children with cerebral palsy. J Neural Eng 12, 046017.

Todorov, E., 2004. Optimality principles in sensorimotor control. Nat Neurosci 7, 907-915.

Torres-Oviedo, G., Macpherson, J.M., Ting, L.H., 2006. Muscle synergy organization is robust across a variety of postural perturbations. J Neurophysiol 96, 1530-1546.

Torres-Oviedo, G., Ting, L.H., 2007. Muscle synergies characterizing human postural responses. J Neurophysiol 98, 2144-2156.

Veeger, H.E., van der Helm, F.C., 2007. Shoulder function: the perfect compromise between mobility and stability. J Biomech 40, 2119-2129.